

Influence of Laying Angles in Reinforcement of Epoxy in Sisal Plain Woven Structures

Palani GOPINATH^{1*}, Paramasivam SURESH²

¹ KSR Institute for Engineering and Technology, Tiruchengode, Namakkal -637215, Tamilnadu, India

² Muthayammal Engineering College, Kakkaveri, Namakkal-637408, Tamilnadu, India

crossref <http://dx.doi.org/10.5755/j02.ms.28608>

Received 06 March 2021; accepted 12 May 2021

This study is about microstructure characterization and understanding the flexural properties of plain-woven sisal fabric reinforced epoxy composites. Vibrational Spectroscopy (FTIR) and SEM (Scanning Electron Microscopy) were used to describe the plain-woven sisal fabric and sisal fiber reinforced epoxy composites. Two laying angles were incorporated into the epoxy resin (10 percent), i.e. (0°/90°) and (0°/45°). To isolate the effect of epoxy type and whether woven sisal fibers were used, an analytical design that is based on (0°/90°) and (0°/45°) orientation used the results. Epoxy treated with woven sisal fibers had a higher tensile (0.62 GPa) and flexural modulus (0.69 GPa) with tensile (17 MPa) and flexural strength (14 MPa) while being applied to a surface that is sloped at 0°/45° and which generates a displacement force of approximately 12 mm and strain 15.8 %. While conventional Weibull failure theory has long been widely used to explain the failure of brittle bulk materials, this new equation integrates that theory with the lay angle effect on flexural strength in plain sisal to calculate flexural strength reinforcement in epoxy. This new method can be applied to any fiber reinforcement, regardless of the type, and in terms of the failure of that reinforcement, which is governed by linear elastic fracture mechanics, and agreement between experimental data sets is excellent. According to our expectations, this theoretical study is going to provide a new method for the advanced strain engineering system to be built using reinforced fibers.

Keywords: sisal, plain woven, tensile strength, flexural strength, Weibull distribution.

1. INTRODUCTION

Normal fiber composites consolidate characteristic filaments, which are separated from plants with a polymer network. Normal fiber composites are otherwise called bio-composite. Presently a day's common fiber polymer composites have been utilized instead of engineered fiber fortified composite on account of biodegradability, light weight, non-risk, shakiness, decreased condition, sulling, negligible exertion, and effortlessness to recyclability [1]. In the early days, some ordinary fiber like coconut fiber and trademark flexible latex were used by the vehicle business. However, now day's ordinary fibers have well-ordered substituted by as of late made man-enhanced fiber because of its execution [2]. The characteristic fiber polymer composites have numerous applications in the electrical field; for instance, cable then connection sheathing and ensuring against electromagnetic interface required the polymer to the mode guiding with a particular true objective to diffuse electrostatic charges [3]. Trademark fiber, for instance, jute, banana, sisal and coir, pineapple leaves, cotton have pulled in light of specialists and technologist for a couple of utilizations like buyer items, insignificant exertion hotel, and regular structures and ordinary polymer composite have better electrical hindrance warm and higher security from facture [4]. On the other way, normal fiber composites have some impediments. Numerous examinations have been done on the capability of normal fiber composites in commonly it demonstrates that the

characteristic fiber polymer has extraordinary strength anyway the composite doesn't accomplish an undefined level from glass fiber composite [4]. Purposes of intrigue and burdens of normal fiber composite have been given underneath [5–7]. Characteristic fiber as a substitution to man-made fiber in fiber fortified composite has extended and opened up current potential results and utilized distinctive concoction alteration on normal fiber which was utilized in common fiber strengthened composite. The substance medicines were improved the situation the enhancement of the hold between the fiber and lattice. The water maintenance of composites was decreased and their mechanical properties are pushed ahead [8]. In a mixture common fiber composite there are at least two distinct kinds of characteristic fiber utilized in a similar framework. Since the composition of the mixture, composite, is determined by the fiber material, fiber presentation, and length of each fiber, the properties of the mixture, composite, differ depending on those variables.

Using the keep running of cross breed mix condition is often used to estimate the consistency and modulus, but for half and half composite, the mechanical properties can be surveyed. The goal of this research project is to investigate the mechanical properties of sisal fiber, and this is done by integrating it into an epoxy resin that is then used to prepare hybrid composites that consist of various volume fractions [9, 10]. Tensile, flexural, and compression testing were performed on the composites to look at their tensile, flexural, and compressive properties.

* Corresponding author. Tel.: +91-4288 274773; fax: +91-4288 274773.
E-mail address: gopipalani@ksriet.ac.in (P. Gopinath)

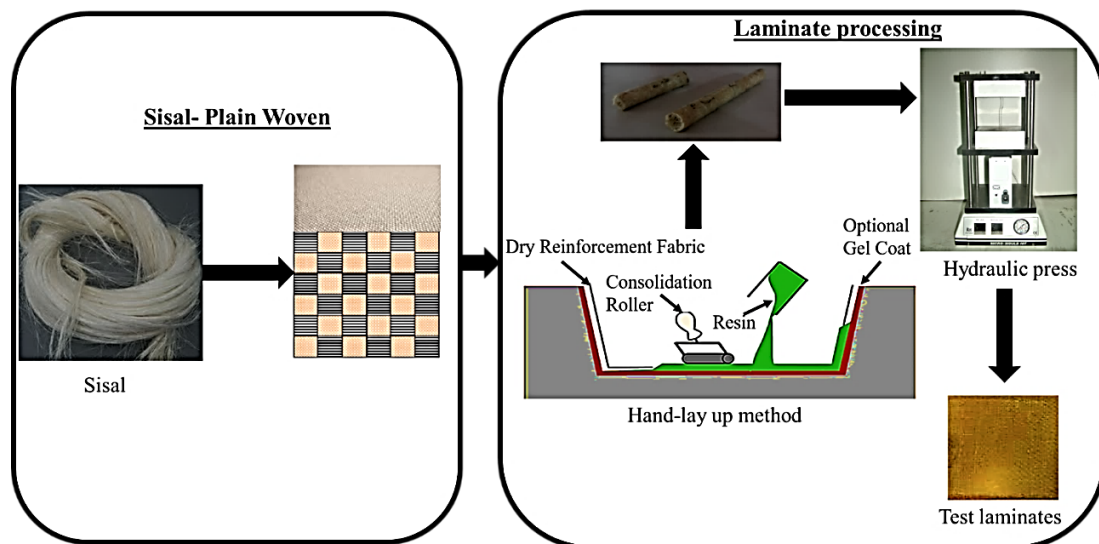


Fig. 1. Schematic diagram of processing and testing of laminates

Several workers [11, 12] have explored the feasibility of using polymer-based composites made of sisal fibers due to the low cost of production of these materials and the various fabrication processes they are compatible with. The processing of these composites was found to be fairly simple and inexpensive. Horizontal and spiral, as well as hoop reinforcement winding, was effective. Fiberglass-epoxy composites were nearly half as solid as sisal-epoxy composites with a tensile strength of about 250–300 MPa. Sisal composites are similar in strength to glass composites because of the low density of the sisal fiber. Sisal-epoxy composites have a unidirectional modulus of around 8.5 GPa. This study proved that integrating one of the available abundant natural fibers in low-cost housing, consumer goods, and civil engineering structures is feasible. When the density of glass fiber composites is considered, it was found that fracture work of ultra-high-modulus polyethylene composites is similar to that of sisal fiber composites, and the fracture toughness of the latter is just 25 % less. Despite of the low strength and modulus of the sisal fiber, the high work of fracture obtained for the sisal fiber composite indicates that the previously proposed statement that natural fiber composite impact behaviour cannot be predicted without considering the helically wound microfibrillar structure of the fiber is correct. Fiber composite durability is related to fiber stress-strain behaviour [13]. High work of fracture is imparted on the composites by materials with high tensile strength and a wide strain tolerance. Epoxy resins provide a wide variety of benefits including low polymerization shrinkage, high mechanical strength, excellent electrical properties, and resistance to chemicals [14]. Also present in epoxy resins are two ring groups located in the middle of the molecule that enable the resin to better withstand both mechanical and thermal stress and, thus, impart the resin with improved stiffness, toughness, and heat resistance.

2. EXPERIMENTAL

2.1. Materials

This study focuses on plain-woven sisal structures flexural properties. Other than linear density (yarn), plain

weave type and reinforcement, the effects of laying angle on the tensile and flexural strength of plain sisals have also been examined. Below are some of the materials and testing methods used to manufacture the formula. All of the sisal rope used in this study was purchased from a company in India called GVR Enterprises. The researcher used a simple loom to create the woven cloth. In terms of tenacity, sisal yarn has an average of 32 cN/tex and a modulus of 723.5 cN/tex.

2.2. Methods-plain sisal yarn

Warp and weft preform were made on a plain loomer using Tex sisal yarn, in warp and weft direction. The woven fabric was 27/22/16 threads/inch with 3.9 mm–4.5 mm thickness (determined from an Askhi fabric thickness indicator, which was having least count of 0.01 mm according to ASTM: D1777). To find out the percentage of crimp on the warp and weft, the measurement was performed, and the results were 9.67 % and 1.2 % respectively. Following this, the samples were used as a starting point for plain sisal laminate preparation. The mechanical properties of sisal and epoxy sisal were evaluated based on the average value of tests conducted on five identical samples. The properties of the plain weave preform are given in Table 1.

Table 1. Plain weave sisal fabric properties

Properties	Sisal
Ends, cm and picks, cm	12
Yarn linear density in Tex	200
Tensile strength in kgs	72
Elongation at warp	21.2 %
Elongation at weft	21.4 %
Areal density in GSM	300

2.3. Preparation of samples

The hand lay-up method was used to render the plain sisal laminates. Preform fabrics were cut to 250 mm × 150 mm and were layered at 0/45/0, 0/90/0 to create a finished sheet. This was achieved by preserving the fiber volume percentage in the ranges of 50–65 %, and measuring with constituent density. To achieve a total

impregnation, 10 % of the epoxy resin was used. This material was laminated using a hot-press that cooked the laminates at 50 °C for two hours under a pressure of 3 bars. Afterwards, the laminated material was baked in an oven at 120 °C for one hour. To test the hypotheses, the experiment's control parameters were selected and specified according to the cause-and-effect diagram. Finally, these selected parameters were explored through a pilot study. For this analysis, we selected a yarn density of 200 tex and 280 GSM, which controls the fiber volume fraction of the plain sisal structure. The most common parameter used when determining reinforcement efficiency is fabric areal density. Then two stages of laying angle were considered: 0/45/0, 0/90/0. After the woven sisal preforms had been produced with the specified pattern as simple, plain sisal fabrics were manufactured by hand lay-up, and then these fabrics were utilized to render woven sisal preforms with the specified pattern on them. To give the molding specifications, the length, width, and thickness of the component must be 300 mm, 160 mm, and 10 mm respectively. When the mold is ready, it is left in place for some time, normally 24 hours, so that it may cure. After that, the pieces are extracted from the mold and sent for testing. Fig. 1. demonstrates the general method of extracting sisal fiber, to the analysis of plain sisal structures.

2.4. Characterization of epoxy reinforced sisal fiber

Perkin Elmer vibrational Spectroscopy was used to distinguish the organic and polymeric compounds. The sisal fiber and its plain sisals were tested in the Frontier Optica model at the highest accuracy. To prevent unnecessary peaks, all samples were fully dried. A Scanning Electron Microscope (SEM) with high efficiency, low-cost instrument (the JOEL JSM 6390LV) was used to research the surface characteristics of the Sisal fiber and its plain sisals. To find out about the behavior of the plain sisals when flexed, a flexural test (ASTM D7264) was performed on both untreated and epoxy-treated samples. A 3-point bending fixture from Instron (model 5967) was used to evaluate the flexural properties of the epoxy plain sisals, with an environmental chamber. For various laying angles (0/45/0, 0/90/0), testing was performed at room temperature (RT) with a holding time of 10 minutes and a loading rate of 1 mm/min.

3. RESULTS AND DISCUSSION

Epoxy treated plain sisal chemical structure and its possible reactions are given in Fig 2. FTIR is an important technique for identifying the different chemical groups and how the epoxy, sisal fiber, and their plain sisals interact. Each material has a specific interaction range in which a specific band dominates. Samples are shown in Fig. 3, and they display the spectra of FTIR for sisal fiber and the epoxy-treated sisal plain sisal. Fig. 3. illustrates the spectra of FTIR, which have the characteristic axial vibration of the hydroxyl group of cellulose at 1630 cm^{-1} and high large peaks about 3200 cm^{-1} are due to the O-H stretching of the lignin and cellulosic structure as well as the hydroxyl group of cellulose (lignin and cellulose together). The out of plane bending of NH gives rise to the slight bump at 1386 cm^{-1} . The strong peak observed between 2775 cm^{-1} and

2912 cm^{-1} in the C-H stretching area of cellulose and hemicelluloses, and known as the aliphatic saturated C-H stretching vibration, results from the aliphatic C-H stretching vibration in cellulose and hemicelluloses [15].

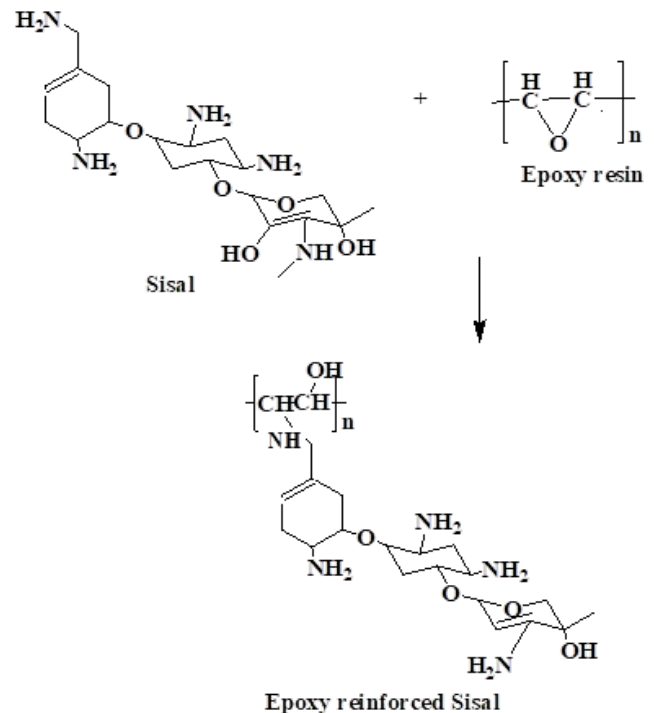


Fig. 2. Epoxy treated sisal chemical structure

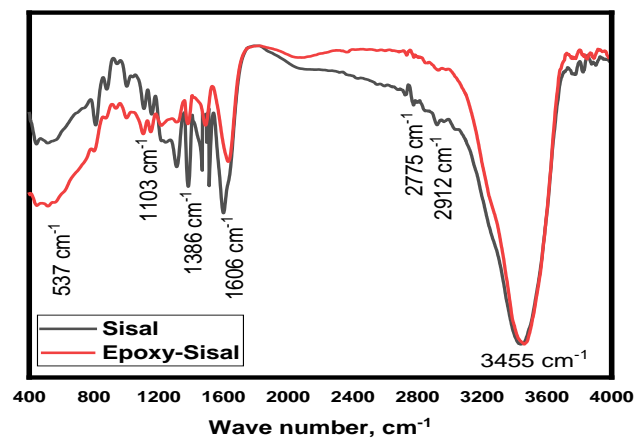


Fig. 3. FTIR spectra of sisal and epoxy-sisal plain sisal structure

3.1. Characterization of epoxy reinforced sisal fiber

The experimental conditions tensile modulus, strength, and ultimate strain values are shown in Table 1. The results of the tensile tests revealed that woven plain sisal fibers in laying angle (45°) epoxy reinforced had a lower tensile modulus than woven plain sisal fibers in (0°/90°) epoxy reinforced, demonstrating the impact of treatment type on this property. In tensile stresses, these epoxies-treated sisal plains showed a high level of interlaminar tension, reducing stiffness. The inter fiber/interlaminar failure theory [16], which is based on the assumption that the limiting microscopic strain in the inter fiber/interlaminar region of the layer governs the failure of epoxies treated sisal plain materials, can explain this mechanism. As shown in Fig. 4

with examples of stress–strain curves, epoxies treated sisal plain with laying angle $[0^\circ/90^\circ]$ had higher tensile strength than those treated with laying angle $[45^\circ]$. The tensile properties of woven sisal fibers reinforced by epoxy were studied, and the tensile strength and modulus of the fibers were highlighted. Because the woven fibers are tightly bonded, the plain sisals reinforced with woven fibers have enormous strength, according to the authors. It's possible that this is due to the stretching nature of woven fibers, which causes strands to break at different times because each fiber can stretch independently and break when it reaches its breaking stress [17]. Plain sisals with woven sisal fibers in laying angle (45°) present multi-axial states of stress in tensile tests, including mutual transverse and shear loadings, which may have a noteworthy impact on the material's failure behavior, lowering tensile strength (Table 2).

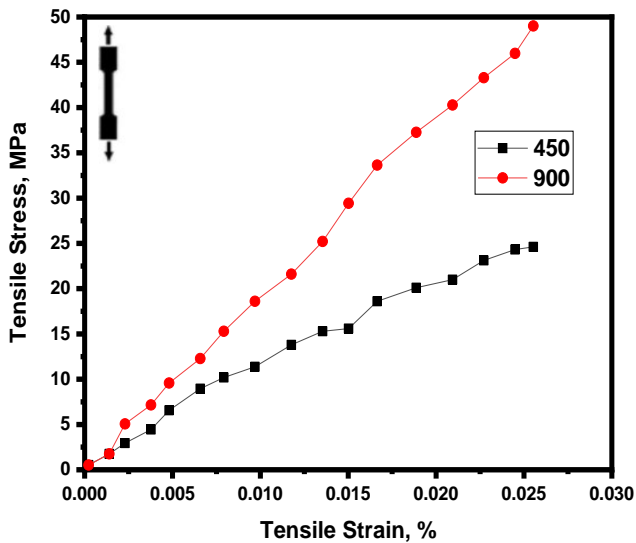


Fig. 4. Tensile stress-strain of epoxy reinforced sisal fibers

3.2. Flexural strength

To investigate the interfacial properties, internal cracks, and internal structure of plain sisal materials, SEM images are taken. In Fig. 5, the SEM images of untreated structure and plain sisal structures treated with epoxy are shown. The fiber in untreated form exhibits significantly lower interface strength than that of the 10% epoxy plain sisal. The epoxy has a less adhered matrix with smoother fibers. This means that there is improved interfacial bonding. These results indicate that the new matrix shows greater fiber/matrix interfacial adhesion because of the modified matrix. Interfacial cracks may be found in some regions, while strong interfacial bonding may be found in other regions [18].

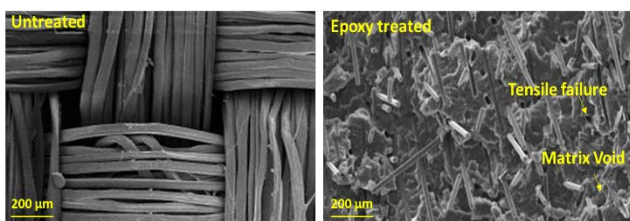


Fig. 5. SEM image of untreated and epoxy treated structures

A key contributing factor to the presence of these cracks is the lower machine-driven properties of the epoxy reinforced sisal. The experimental conditions' flexural modulus, flexural strength, and displacement values are shown in Table 3.

Table 2. Tensile parameters of epoxy reinforced plain sisal

Laying angle of epoxy sisal plain	Tensile modulus, GPa	Tensile strength, MPa	Strain, %
$0^\circ/0^\circ$	0.69 ± 0.04	14.21 ± 0.30	11.45 ± 0.81
$0^\circ/45^\circ$	0.65 ± 0.01	17.36 ± 0.41	15.89 ± 0.32
$0^\circ/90^\circ$	0.54 ± 0.02	11.10 ± 0.55	20.72 ± 0.42

Also, the epoxy treated sisal woven fibers oriented $[0^\circ/45^\circ]$ outperformed the other group, which had fibers at $(0^\circ/90^\circ)$. The plain sisal structure may have taken on slightly different characteristics based on these breaks among the yarns, the wettability of the fibers, also the insignificant dissimilarities in temperature throughout the thermal zones during the polymer melting process (Fig. 5). Tensile, shear stresses and compression are applied at the same time during flexural testing. Fibers oriented at 45° develop shear strain in the matrix.

Table 3. Flexural parameters of epoxy reinforced plain sisal

Laying angle of epoxy sisal plain	Flexural modulus, GPa	Flexural strength, MPa	Displacement, mm
$0^\circ/0^\circ$	0.62 ± 0.04	15.89 ± 0.91	9.31 ± 0.61
$0^\circ/45^\circ$	0.69 ± 0.02	13.85 ± 0.23	11.83 ± 0.46
$0^\circ/90^\circ$	0.51 ± 0.03	13.91 ± 0.72	11.54 ± 0.73

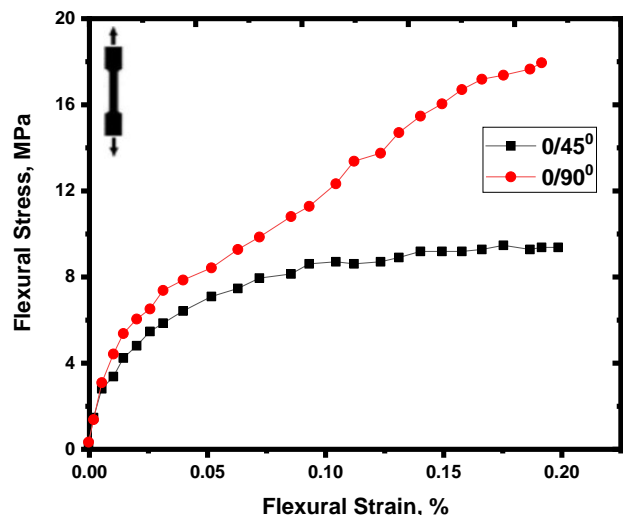


Fig. 6. Flexural stress-strain of epoxy reinforced sisal fibers

This type of material tends to have a strong shear stress, which influences the flexural test results (Fig. 6). As long as the interfacial bonding is insufficient, the delamination size grows in response to applied stress, with no relation to the amount of stress. There is an increase in stress, which may result in layers detaching, decreasing the global stiffness [19]. As demonstrated in Fig. 7, epoxy-reinforced plain sisal has an elastic region in which lines are more inclined. Assumed to be predominant in these tests is shear failure, when the load-displacement curve steepens before leveling

off to zero. We find that compared to 0° and 90°, a higher incidence of reinforcement fiber performance, because the fibers that are oriented at 90° (upright to the test) are less rigid under flexural stress (Fig. 7). Because of the interlaminar tension in tensile stresses, the stiffness of this plain sisal-reinforced epoxy mixture was reduced. Interfiber/interlaminar failure is responsible for this mechanism [20].

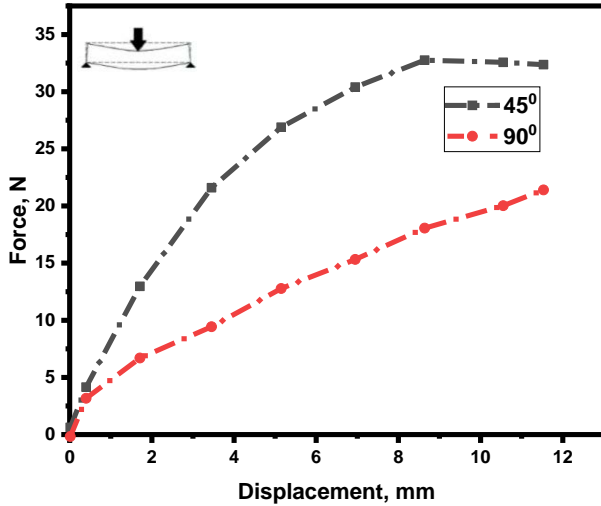


Fig. 7. Flexural Force-Displacement curves of epoxy reinforced plain sisal

3.3. Mechanical strength-Weibull distribution

When it comes to structural applications, it is critical to have an accurate idea of the material's machine-driven performance below the service conditions. In the case of epoxy treated sisal, numerous distortion/micro-let down mechanisms, such as the development of twist bands, shear points, limited flexure, micro-fastening, etc., will occur as a result of multiple mechanisms acting in concert. Failure mechanisms in the flow matrix, reinforcement, and interface/interphase are all interconnected. The four typical failure modes in these materials are fiber fragmentation, matrix cracking, pull-out, and debonding at the fiber-matrix interface. In the machine-driven performance (strength) of epoxy treated sisal, the Weibull probability distribution function can be used to successfully model the distribution. simulated stress (s) and strain (e):

$$\sigma = E\epsilon \exp\left[-\left(\frac{E\epsilon}{\sigma_0}\right)^\beta\right]; \quad (1)$$

$$\ln\left[\ln\left(\frac{E\epsilon}{\sigma_0}\right)\right] = \beta \ln(E\epsilon) - \beta \ln(\sigma_0), \quad (2)$$

where σ is the simulated stress of material; ϵ is the simulated strain of material; β is the shape parameter of material; E is the Elastic modulus of material i parallel to the direction of applied load; σ_0 is the scale parameter of material. Data on experimental stress (s) and strain (e) is applied to draw a graph between $\ln(E\epsilon)$ and $\ln(E\epsilon/\sigma)$, which results in a straight line with a slope of β and an intercept of $\beta \ln(\sigma)$. After finding the value of β , one can determine the value of σ_0 . A figure (illustrated in Fig. 8) illustrates the Weibull linear fittings used to fit experimental epoxy reinforced plain sisal data at two different laying angles. Careful inspection of Fig. 8 shows that as the epoxy content in the composite laminates

increases, the flexural strength scale parameter (σ) follows a similar trend. Conversely, it was found that the shape parameter (β) steadily decreased as epoxy was added. These results indicate that as the epoxy content increases, the degree of scatteredness of the plain sisal becomes greater.

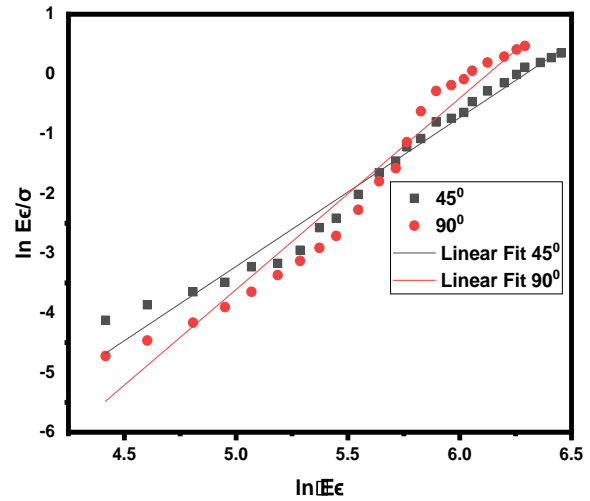


Fig. 8. Weibull linear fittings at different laying angles

4. CONCLUSIONS

To study the tensile and flexural properties of epoxy reinforced plain sisal fabric, the effect of laying angle was analysed and evaluated. It is possible to create plain sisals in a controlled process using hot compression moulding with controlled pressure and temperature. The epoxy-reinforced woven sisal has a flexural property in which untreated woven sisal fibers are oriented at 90° and 45°. Sisal oriented at (45°) demonstrates the greatest tensile and flexural strength. Flexural and tensile properties of plain sisal with a raising drift of β and consequently a lowering grade of sprinkle in the strength deteriorate, leading to an increase in the scatter in the Weibull model predictions as well as an increased risk of problems in tensile and flexural properties.

REFERENCES

1. **Obiukwu, O.O., Igboekwe, J.** Mechanical, Morphological Properties and Chemical Resistance of Filled Rattan Wastes Powder Epoxy Composites *Iranian (Iranica) Journal of Energy & Environment* 11 (4) 2020: pp. 320–329. <https://doi.org/10.5829/ijee.2020.11.04.10>
2. **Roy, K., Debnath, S.C., Tzounis, L., Pongwisuthiruchte, A., Potiyaraj, P.** Effect of Various Surface Treatments on The Performance of Jute Fibers Filled Natural Rubber (Nr) Composites *Polymers* 12 (2) 2020: pp. 369–383. <https://doi.org/10.3390/polym12020369>
3. **Touati, Z., de Hoyos-Martinez, P.L., Blhanché-Bensemra, N., Charrier-El Bouhtouri, F.** Influence of Different Diss Fiber Treatments Over the Properties of Poly Propylene/Recycled and Regenerated Low-Density Polyethylene Based Biocomposites *Journal of Polymers and The Environment* 29 2021: pp. 291–303. <https://doi.org/10.1007/s10924-020-01877-7>
4. **Verma, A., Parashar, A., Jain, N., Singh, V.K., Rangappa, S.M., Siengchin, S.** Surface Modification

Techniques for The Preparation of Different Novel Biofibers for Composites in Biofibers and Biopolymers for Biocomposites *Springer, Cham.* (1) 2020: pp. 1–34. https://doi.org/10.1007/978-3-030-40301-0_1

5. **Taban, E., Khavanin, A., Faridan, M., Samaei, S.E., Samimi, K., Rashidi, R.** Comparison of Acoustic Absorption Characteristics of Coir and Date Palm Fibers: Experimental and Analytical Study of Green Composites *International Journal of Environmental Science and Technology* 17 (1) 2020: pp. 39–48. <https://doi.org/10.1007/s13762-019-02304-8>
6. **Arul, M., Sasikumar, K.S.K., Sambathkumar, M., Gukendran, R., Saravanan, N.** Mechanical and Fracture Study of Hybrid Natural Fiber Reinforced Composite–Coir and Sugarcane Leaf Sheath *Materials Today: Proceedings* 33 2020: pp. 2795–2797. <https://doi.org/10.1016/j.matpr.2020.02.677>
7. **Reddy, B.M., Kumar, G.S., Reddy, Y.V.M., Reddy, P.V., Reddy, B.C.M.** Study on the Effect of Granite Powder Fillers in Surface-Treated Cordia Dichotoma Fiber-Reinforced Epoxy Composite *Journal of Natural Fibers* 2020: pp. 1–16. <https://doi.org/10.1080/15440478.2020.1789022>
8. **Prabhu, L., Krishnaraj, V., Sathish, S., Gokulkumar, S., Karthi, N., Rajeshkumar, L., Balaji, D., Vigneshkumar, N., Elango, K.S.** A Review on Natural Fiber Reinforced Hybrid Composites: Chemical Treatments, Manufacturing Methods and Potential Applications *Materials Today: Proceedings* 45 (9) 2021: pp. 8080–8085. <https://doi.org/10.1016/j.matpr.2021.01.280>
9. **Singh, S.B., Vummadiseti, S., Chawla, H.** Development and Characterisation of Novel Functionally Graded Hybrid of Carbon-Glass Fibres *International Journal of Materials Engineering Innovation* 11 (3) 2020: pp. 212–243. <https://doi.org/10.1504/IJMATEI.2020.108883>
10. **Guo, G., Kethineni, C.** Direct Injection Molding of Hybrid Polypropylene/Wood-Fiber Composites Reinforced with Glass Fiber and Carbon Fiber *The International Journal of Advanced Manufacturing Technology* 106 (1) 2020: pp. 201–209. <https://doi.org/10.1007/s00170-019-04572-7>
11. **Zilio, L., Dias, M., Santos, T., Santos, C., Fonseca, R., Amaral, A., Aquino, M.** Characterization and Statistical Analysis of The Mechanical Behavior of Knitted Structures Used to Reinforce Composites: Yarn Compositions and Float Stitches *Journal of Materials Research and Technology* 9 (4) 2020: pp. 8323–8336. <https://doi.org/10.1016/j.jmrt.2020.05.089>
12. **Baranov, A., Sommerhoff, F., Duchemin, B., Curnow, O., Staiger, M.P.** Toward a Facile Fabrication Route for All-Cellulose Composite Laminates Via Partial Dissolution in Aqueous Tetrabutylphosphonium Hydroxide Solution *Composites Part A: Applied Science and Manufacturing* 140 2021: pp. 106148. <https://doi.org/10.1016/j.compositesa.2020.106148>
13. **Zeng, J.J., Ye, Y.Y., Gao, W.Y., Smith, S.T., Guo, Y.C.** Stress-strain Behavior of Polyethylene Terephthalate Fiber-Reinforced Polymer-Confined Normal-, High-and Ultra-High Strength Concrete *Journal of Building Engineering* 30 2020: pp. 101243. <https://doi.org/10.1016/j.job.2020.101243>
14. **Peerzada, M., Abbasi, S., Lau, K.T., Hameed, N.** Additive Manufacturing of Epoxy Resins: Materials, Methods, and Latest Trends *Industrial & Engineering Chemistry Research* 59 (14) 2020: pp. 6375–6390. <https://doi.org/10.1021/acs.iecr.9b06870>
15. **Cecchi, R.R.R., Passos, A.A., de Aguiar Neto, T.C., Silva, L.A.** Banana Pseudostem Fibers Characterization and Comparison with Reported Data on Jute and Sisal Fibers *Sn Applied Sciences* 2 (1) 2020: pp. 1–6. <https://doi.org/10.1007/s42452-019-1790-8>
16. **Liu, H., Liu, J., Ding, Y., Zhou, J., Kong, X., Blackman, B.R., Kinloch, A.J., Falzon, B.G., Dear, J.P.** Effects of Impactor Geometry on the Low-Velocity Impact Behaviour of Fibre-Reinforced Composites: An Experimental and Theoretical Investigation *Applied Composite Materials* 27 (5) 2020: pp. 533–553. <https://doi.org/10.1007/s10443-020-09812-8>
17. **Hui, C.Y., Liu, Z., Phoenix, S.L., King, D.R., Cui, W., Huang, Y., Gong, J.P.** Mechanical Behavior of Unidirectional Fiber Reinforced Soft Composites *Extreme Mechanics Letters* 35 2020: pp. 100642. <https://doi.org/10.1016/j.eml.2020.100642>
18. **Cui, W., King, D.R., Huang, Y., Chen, L., Sun, T.L., Guo, Y., Saruwatari, Y., Hui, C.Y., Kurokawa, T., Gong, J.P.** Fiber Reinforced Visco-Elastomers Show Extraordinary Crack Resistance That Exceeds Metals *Advanced Materials* 32 (31) 2020: pp. 1907180. <https://doi.org/10.1002/adma.201907180>
19. **Plocher, J., Panesar, A.** Effect of Density and Unit Cell Size Grading on the Stiffness and Energy Absorption of Short Fibre-Reinforced Functionally Graded Lattice Structures *Additive Manufacturing* 33 2020: pp. 101171. <https://doi.org/10.1016/j.addma.2020.101171>
20. **David Müzel, S., Bonhin, E.P., Guimarães, N.M., Guidi, E.S.** Application of the Finite Element Method in the Analysis of Composite Materials: A Review *Polymers* 12 (4) 2020: pp. 818. <https://doi.org/10.3390/polym12040818>



© Gopinath et al. 2022 Open Access This article is distributed under the terms of the Creative Commons Attribution 4.0 International License (<http://creativecommons.org/licenses/by/4.0/>), which permits unrestricted use, distribution, and reproduction in any medium, provided you give appropriate credit to the original author(s) and the source, provide a link to the Creative Commons license, and indicate if changes were made.